Dipping Time and Annealing Effect on TiO_2 Thin Films Grown by Sol-Gel Dip Coating Method (SGDC)

Samet UYSAL and Aytunç ATEŞ

Metallurgy and Materials Engineering/ Faculty of Engineering and Natural Sciences, Ankara Yıldırım Beyazıt University

aates@ybu.edu.tr *Email of the corresponding author*

Abstract – TiO_2 semiconductor is highly functional materials for solar cell applications such as photo catalysis and photovoltaics owing to the superior opto electrical properties and chemical stability. Annealing temperature and dipping time effect on TiO_2 thin films grown by SG-DC method were investigated. The solution was prepared using Titanium (IV) Isopropoxide (TTIP), ethanol and acetone solutions are used. TiO_2 thin films grown by Dip Coating method on glass substrates with 5, 10, 20 seconds dipping time at a speed of 0.5 cm/s and annealed at temperatures from 300°C to 600°C. Structural characterizations of TiO_2 thin films were investigated by X-ray Diffraction (XRD) and Scanning Electron Microscope (SEM), and optical properties were investigated by UV-Spectroscopy. According to XRD analysis, TiO2 anatase phase observed for unannealed and annealed at 300 ^{0}C thin films. The polycrystalline peaks observed after 400 ^{0}C and the peaks intensity, sharpness and narrowing are decreased with increasing temperature. From the absorption data, the band gap values (Eg) decreased from 3.31 to 3.06 eV with increasing annealing temperature and increase with increasing dipping time. The SEM analysis show that TiO_2 nanoparticles grown spherical shape. It was determined that the dipping time and annealing temperature cause changing in the characteristic properties of TiO_2 thin films.

Keywords – Tio_2, Sol-Gel, Dip Coating, Annealing Temperature, Dipping Time

I. INTRODUCTION

Titanium dioxide, which is among the nanostructured metal-oxide materials, has been used frequently in research due to its different chemical, electrical and optical properties. TiO_2 is highly functional for photocatalysis and photovoltaic applications due to its superior optoelectronic properties and outstanding chemical stability [1]. Main thin film coating and growth techniques are Chemical Vapor Deposition (CVD), sol-gel, electrochemical deposition, Physical Vapor Deposition (PVD), thermal spray methods [2].

Molecular precursors are hydrolized and condensed in the process of sol-gel synthesis, which has been applied to produce inorganic compounds in a variety of methods. The most important advantage of the sol-gel technique is that it can be performed without the need for conditions such as high pressure and temperature. Unlike solid-state processes, the sol-gel process offers molecular control of the reaction pathway during the transformation of precursors species to the final product. Therefore, the sol-gel process can produce nanoparticles of very high purity and homogeneity, uniform crystal morphology, and well-defined. The basic steps of the sol-gel process are hydrolysis of the precursor in a suitable solvent with or without a catalyst to form sol, gelation by polymerization reactions, aging to form a stable structure, drying to

remove excess solvent, and annealing to remove organics and crystallize solid material. In the sol-gel method, the precursor concentration, reaction conditions, aging time, coating type, annealing temperature and time determine the properties of the film [3].

Karabay et al. grew TiO_2 thin films with the sol-gel method, examined the effects of annealing temperature, and observed the transformation from amorphous structure to anatase structure [4]. Mechiakha et al. stated that the films annealed at 400-800 ^{0}C were seen in the anatase phase, at 1000 ^{0}C were in the rutile-anatase phase, and at 1200 ^{0}C were seen in the rutile phase [5]. Bakri et al. reported an increase in anatase (101) peak intensity, decrease in FWHM, increase in crystallite size and surface roughness with increasing annealing temperature of TiO_2 films grown on glass substrate by sol-gel technique [6]. Senthil et al. investigated the optical properties of thin films using the transmittance spectra, and it was seen that the optical band gap decreased from 3.71 eV to 3.19 eV with increasing annealing temperature [7]. Ranjitha et al. noted that with increasing annealing temperature, the absorption thresholds shift to longer wavelengths [8]. Touam et al. grew TiO_2 thin films by sol gel dip coating (SGDC) method and examined the effects of dipping speed. They observed a change in the optical and structural properties of the film with increasing dipping speed [9].

The annealing temperature and dipping time on TiO_2 thin films characteristic properties as optical and structural have been investigated.

II. MATERIALS AND METHOD

Titanium (lV) isopropoxide ($Ti[OCH(CH_3)_2]_4$) (TTIP), ethanol (C_2H_5OH) and acetone (C_3H_6O) were used as a precursor, solvent and stabilizer, respectively to prepare the sol-gel solution. 15 ml of ethanol was added to 10 ml of titanium isopropoxide and mixed for 10 minutes. Acetone (2 ml) and ethanol (4 ml) were mixed and slowly added to the first solution and stirred at room temperature for 90 minutes. The cleaned glass substrates were immersed in the prepared TiO_2 sol-gel solution crosswise at a speed of 0.5 cm/sec, grown for 5, 10, 20 seconds, and removed from solution at the same speed. The films were dried at 100 °C for half an hour and annealed at 300, 400, 500 and 600 ^{0}C during 1 hour. The crystalline structure was characterized by an XRD (Miniflex 600, Rigaku) in 2θ range from 20^0 to 70^0 by 2 min^{-1} steps operating at 40 kV accelerating voltage and 15 mA current using Cu Ka radiation source. SEM (FlexSEM 1000 II, HITACHI) was used to study the shapes of nanoparticles, uniformity and homogeneity of the film. UV-Vis spectroscopy was used to investigate the optical properties of the films.

III. RESULTS AND DISCUSSION

Figure 1,2 shows scanning electron microscope morphology of TiO_2 nanostructures at magnification 1000×, and 10000x for unannealed and annealed at 300˚C, 400˚C, 500˚C and 600˚C. They cooled naturally in the air. It was observed that the surface morphology of the nanostructure films shows good uniformity, homogeneity, smooth with cracks and holes. Figure 3 show the SEM image of thin film for 5, 10, 20 s dipping times.

The particles are approximately in spherical form. Similar structures have been seen in previous studies [10-12]. By increasing the annealing temperature from 300˚C up to 600˚C, it was found that the size and the agglomeration becomes increasingly attenuated. The unannealed film shows a porous and homogeneously cracked surface. With the annealing of the films, larger cracks were observed on the surface. All films exhibit larger island-like structures and these decrease with increasing annealing temperature.

It was observed that the grain size increased with the increase in the annealing temperature. Grain boundaries are clearly seen in the SEM micrographs. The result shows that all samples were agglomerated with an average grain size, approximately. The agglomeration may be caused by several factors such as the presence of capillary absorption, solid bridge, Van der Waals and hydrogen bond [13]. Brinker and Scherer reported that the small particles inclined to agglomerate due to the high surface energy, coalescing the particles together and formed larger particles. [14].

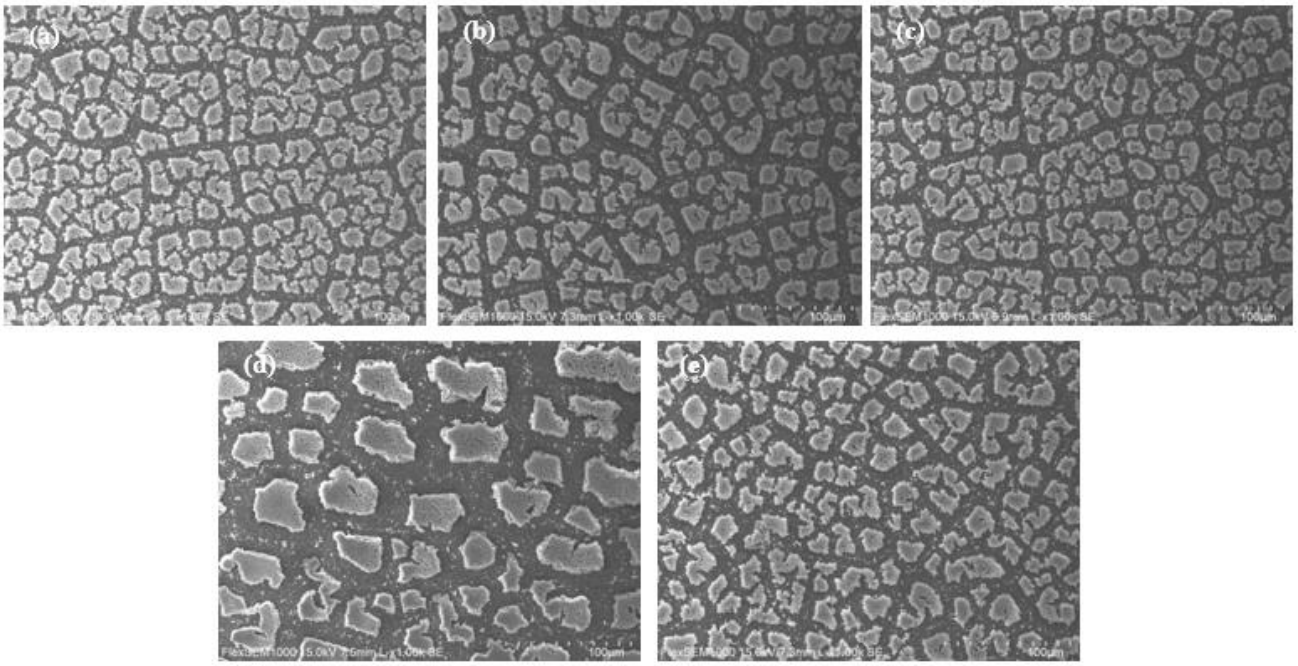

Fig. 1 SEM micrograph (1kx) of TiO_2 thin films unannealed (a), annealed at 300 (b), 400 (c), 500 (d), 600 (e).

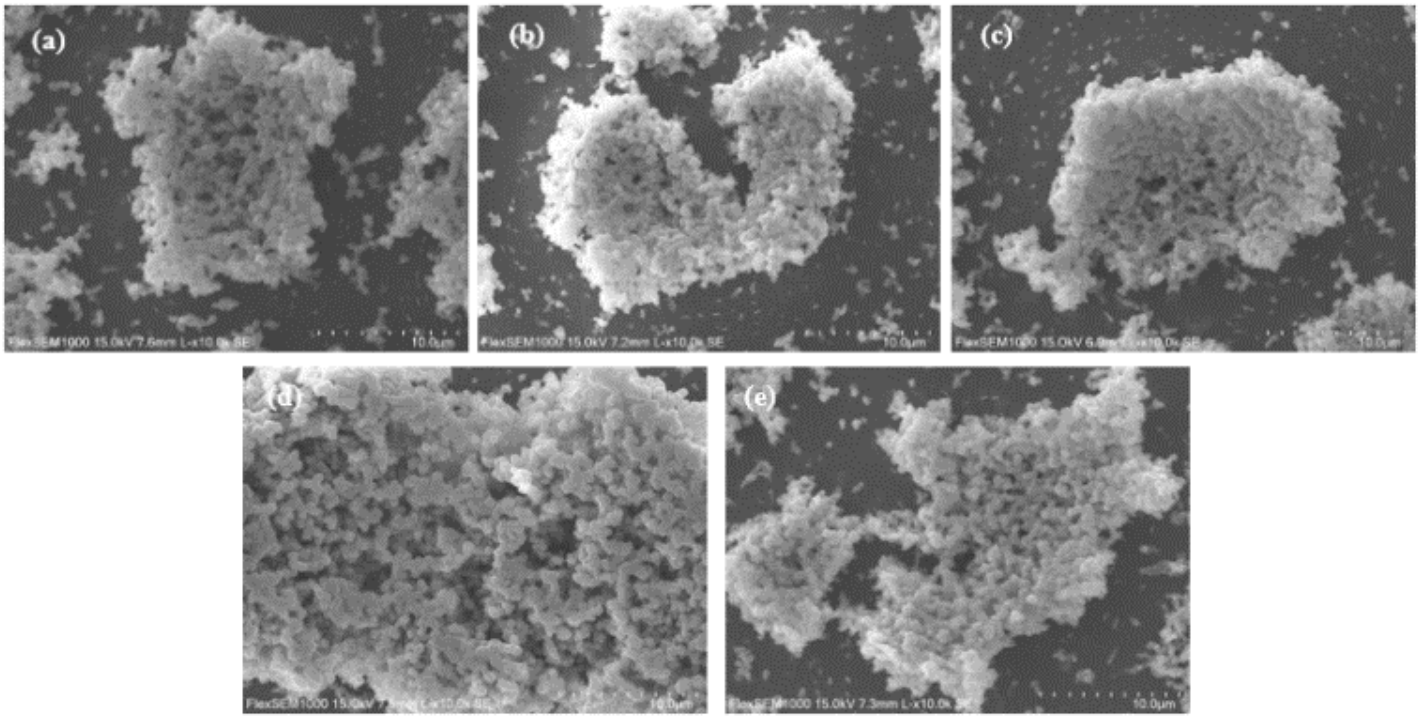

Fig. 2 SEM micrograph (10kx) of TiO_2 thin films unannealed (a), annealed at 300 (b), 400 (c), 500 (d), 600 (e).

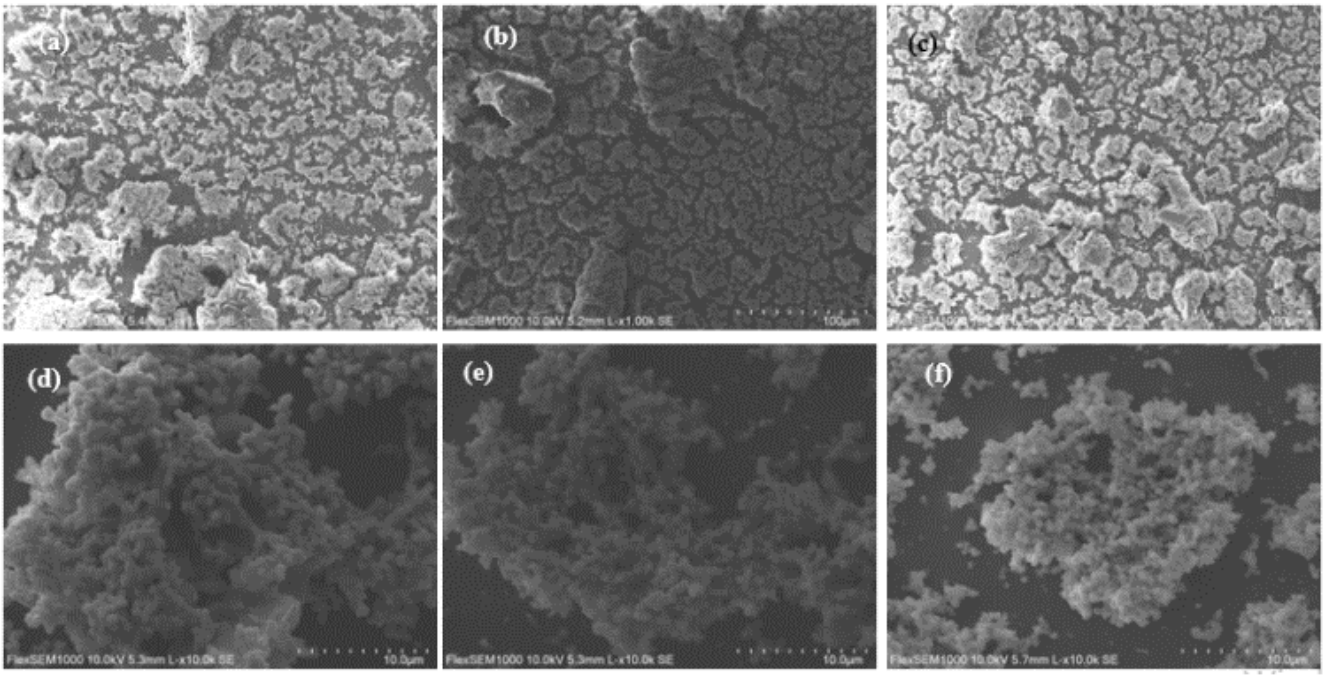

Fig.3 SEM image of thin film for 5, 10, 20 s dipping times.

The XRD patterns of TiO_2 thin films for unannealed and annealed at 300, 400, 500, 600 ^oC were given in figure 5. Unannealed and annealed at 300 ^oC exhibited amorphous structures. However, XRD peaks began to appear for annealed at 400, 500 and 600 ^oC thin films.

The grain size was calculated using the full width at half maximum (FWHM) of the intense (1 0 1) diffraction peak of anatase TiO_2 according to the Scherer equation [15];

$$D = \frac{k\lambda}{\beta cos\theta} \quad (2)$$

Where D stands for the crystallite size in nanometers, k for the incident radiation's wavelength in nanometers, k = 0.90, a constant, h for the measured Bragg angle in radians, and b for the FWHM in radians. Table 1 provides the estimated crystallite size of the films for unannealed and annealed at 400–600 ^oC.

Table 1 Some parameters obtained from XRD spectrum of TiO_2 thin films annealed at 400, 500, 600 ^0C.

Annealed temperature (^0C)	**Intensity**	**FWHM (^{o})**	**2θ (^{o})**	**Crystal size (nm)**
400	2850	0.433	25.30	19.22
500	3203	0.418	25.28	19.91
600	3405	0.403	25.26	20.63

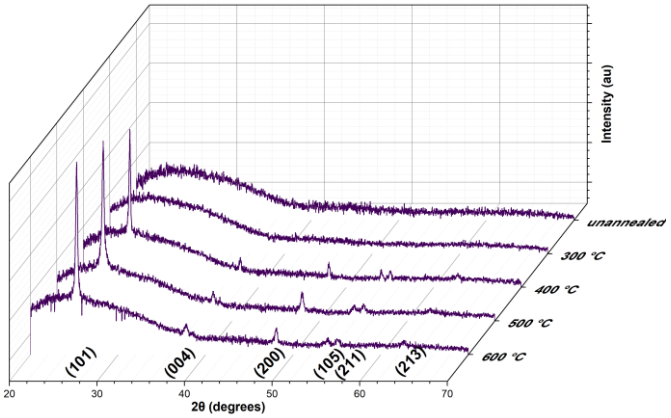

Fig. 5 The XRD pattern of the TiO_2 film unannealed and annealed at 300, 400, 500, 600 ^0C.

It was determined that the films changed from amorphous to polycrystalline structure when annealed at 400 ^oC and the peak intensities increased with the increase of annealing temperature. At 400, 500, 600 ^oC the peaks of the anatase phase became well defined and were matched with (JCPDS 21-1272).

Figure 5 shows the absorption spectra of the unannealed and annealed at 300-600 ^0C for TiO_2 thin films. All films show high absorption in the UV region of the wavelength, decreasing in the near-visible range. This is related to the electron's transition from the valence band to the conduction

band and the generation of the pair of electrons and holes [16].

Figure 6 shows the absorption spectra of the TiO_2 thin films for different dipping time of 5, 10, 20 seconds. Figure 7 shows the $(\alpha h\nu)^2$ vs hv plot from absorption data for TiO_2 thin films for unannealed and annealed at 300-600 ^oC. The optical band gap was calculated by using the below Tauc plot with using below equation [17];

$$\alpha h\nu = A(h\nu - Eg) \quad (1)$$

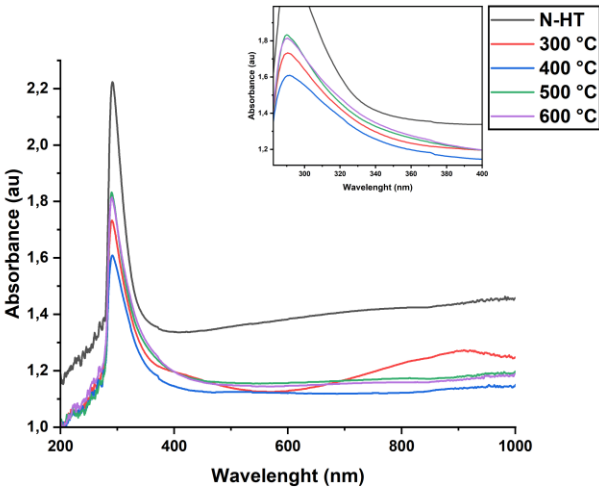

Fig.5 shows the absorption spectra of the unannealed and annealed at 300-600 0C for TiO2 thin films.

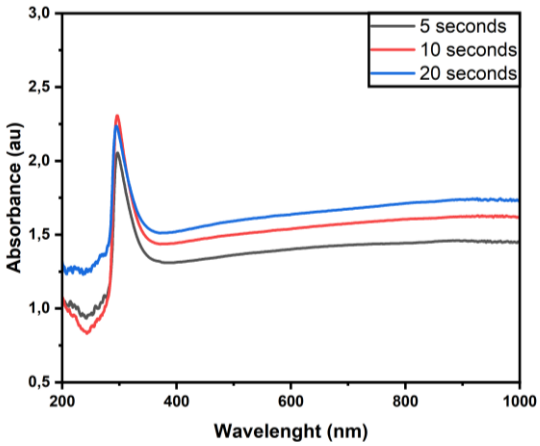

Fig. 6 UV-VIS measurement of TiO2 thin films for dipping time 5, 10, 20 s.

It was seen that the bandgap values of the thin films decreased from 3.31 to 3.06 with increasing annealing temperature (Table. 2). This may be due to the the effect of increases of grain sizes with increasing annealing temperatures. An increase of the grain sizes has weakened the quantum size effects and thus, lead to the decreased in the band gap energy [18]. These results are agreement with the XRD results (see Table 1). Densely packed crystalline structures of the films cause a decreasing in band gap values [19]. As seen in figure 8, the band gaps of the films as a function of dipping time for 5, 10, 20 seconds are calculated as 3.28, 3.31, 3.37 eV, respectively (Table. 3). The higher band gap observed in our case can be associated with the nano crystalline nature of the films [20]. This behavior is attributed to the variance in film composition and phase formations. [21]. If we explain the expansion of Eg with the well-known Burstein-Moss (BM) effect [22], First, the lowest states in the conduction band are blocked and transitions can only occur at higher energy levels in the conduction band. This effect is often observed in degenerated serniconductors. Thus, it is assumed that the optical band gap's blue shift indicates an increase in carrier density. [23].

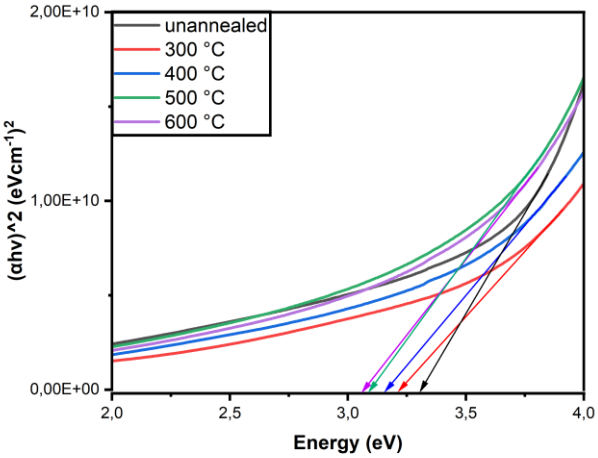

Fig. 7 $(\alpha h\nu)^2$ as a function of hv for the TiO_2 film unannealed and annealed 300, 400, 500, 600 ^0C.

Table 2 Bandgap of the TiO_2 films unannealed and annealed 300, 400, 500, 600 ^0C

Annealed temperature (^0C)	**Unannealed**	**300**	**400**	**500**	**600**
Bandgap (eV)	3.31	3.21	3.16	3.09	3.06

Table 3 Bandgap of the TiO_2 films for dipping time 5, 10, 20 s.

Dipping time (s)	**5**	**10**	**20**
Bandgap (eV)	3.28	3.31	3.37

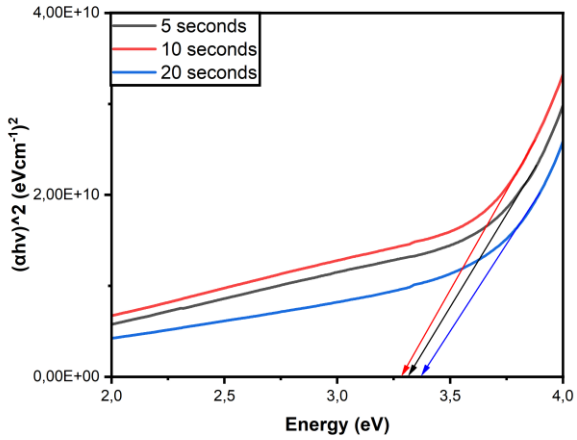

Fig. 8 $(\alpha h\nu)^2$ as a function of hν for the TiO_2 films for dipping time 5, 10, 20 s.

IV. CONCLUSION

TiO_2 nanostructure film has been successfully synthesized by SGDC method. TiO_2 thin films grown by Sol-gel/Dip Coating (SGDC) method were investigated. The solution was prepared using Titanium (IV) Isopropoxide (TTIP), ethanol and acetone solutions are used. TiO_2 films were grown by Dip Coating method on glass substrates with 5, 10, 20 seconds dipping time at a speed of 0.5 cm/s and annealed at temperatures from 300°C to 600°C. According to XRD analysis, TiO_2 anatase phase observed for unannealed and annealed at 300 ^{0}C thin films with amorphous structure. The polycrystal peaks observed after 400 ^{0}C and the peaks intensity, sharpness and peak's narrowing are decreased with increasing temperature. From the absorption data, the band gap values decreased from 3.31 to 3.06 eV with increasing annealing temperature. The band gap values increased with increasing dipping time ~~too~~. The SEM analysis show that TiO_2 nanoparticles grown spherical shape. It was determined that the dipping time and annealing temperature cause changing in the characteristic properties of TiO_2 thin films.

ACKNOWLEDGMENT

This study was financially supported by Ankara Yıldırım Beyazıt University Scientific Research Fund [project code: FYL-2022-2427]

REFERENCES

[1] H. He, C. Liu, K.D. Dubois, T. Jin, M.E. Louis, & G. Li, "Enhanced charge separation in nanostructured TiO2 materials for photocatalytic and photovoltaic applications," *Industrial & engineering chemistry research*, *51*(37), 11841-11849, 2012.

[2] Abegunde, O. O., Akinlabi, E. T., Oladijo, O. P., Akinlabi, S., & Ude, A. U., "*Overview of thin film deposition techniques*," *AIMS Materials Science* 6.2, 174-199, 2019.

[3] Ş. Toygun, G. Köneçoğlu, And Y. Kalpakli. "General principles of sol-gel." *Sigma Journal of Engineering and Natural Sciences* 31.4 (2013): 456-476.

[4] Karabay, I., Aydın Yüksel, S., Ongül, F., Öztürk, S., & Aslı, M. "Structural and Optical Characterization of TiO_2 Thin Films Prepared by Sol-Gel Process." *Acta Physica Polonica A* 121.1 (2012): 265-267.

[5] Mechiakh, R., Sedrine, N. B., Chtourou, R., & Bensaha, R. "Correlation between microstructure and optical properties of nano-crystalline TiO2 thin films prepared by sol–gel dip coating." *Applied Surface Science* 257.3 (2010): 670-676.

[6] Bakri, A. S., Sahdan, M. Z., Adriyanto, F., Raship, N. A., Said, N. D. M., Abdullah, S. A., & Rahim, M. S., "Effect of annealing temperature of titanium dioxide thin films on structural and electrical properties." *AIP conference proceedings*. Vol. 1788. No. 1. AIP Publishing LLC, 2017.

[7] Senthil, T. S., Thambidurai, M., Muthukumarasamy, N., & Balasundaraprabhu, "Structural And Optical Investigations On Nanocrystalline Tio2 Thin Films Prepared By Sol–Gel Spin Coating Technique." International Journal of Nanoscience 9.04 (2010): 355-358.

[8] Ranjitha, A., Muthukumarasamy, N., Thambidurai, M., Balasundaraprabhu, R., & Agilan, S. "Effect of annealing temperature on nanocrystalline TiO2 thin films prepared by sol–gel dip coating method." *Optik* 124.23 (2013): 6201-6204.

[9] Touam, T., Atoui, M., Hadjoub, I., Chelouche, A., Boudine, B., Fischer, A., ... & Doghmane, A. "Effects of dip-coating speed and annealing temperature on structural, morphological and optical properties of sol-gel nano-structured TiO2 thin films." *The European Physical Journal Applied Physics* 67.3 (2014): 30302.

[10] Hafizah, Nor, and Iis Sopyan. "Nanosized TiO2 photocatalyst powder via sol-gel method: effect of hydrolysis degree on powder properties." *International Journal of Photoenergy* 2009 (2009).

[11] Yahaya, M. Z., Azam, M. A., Teridi, M. A. M., Singh, P. K., & Mohamad, A. A. Recent characterisation of sol-gel synthesised TiO2 nanoparticles. *Recent applications in Sol-Gel synthesis*, 109-129, (2017).

[12] Amole, S., Awodele, M. K., Adedokun, O., Jain, M., & Awodugba, A. O. (2019). Sol-Gel Spin Coating Synthesis of TiO2 Nanostructure and Its Optical Characterization. *Journal of Materials Science and Chemical Engineering*, *7*(6), 23-34.

[13] Su, Y., Xiao, Y., Li, Y., Du, Y., & Zhang, Y. (2011). *Preparation, photocatalytic performance and electronic structures of visible-light-driven Fe–N-codoped TiO2 nanoparticles*. Materials Chemistry and Physics, 126, 76176

[14] Brinker, C. J., & Scherer, G. W. (1990). Sol-gel science: the physics and chemistry of sol-gel processing; Academic Pr.
[15] Yunus Akaltun , M.Ali Yıldırım , Aytunç Ateş , Muham met Yıldırım Zinc concentration effect on structural, optical and electrical properties of Cd1−xZnxSe thin films Materials Research Bulletin Volume 47, Issue 11, November 2012, Pages 3390-3396
[16] Tański, T., Matysiak, W., Kosmalska, D., & Lubos, A. "Influence of calcination temperature on optical and structural properties of TiO2 thin films prepared by means of sol-gel and spin coating." *Bulletin of the Polish Academy of Sciences: Technical Sciences* (2018): 151-156.
[17] Yasemin Pepe , MehmetAli Yildirim , Ahmet Karatay , Aytunc Ate c, Huseyin Unver , Ayhan Elmali *The effect of doping and annealing on the nonlinear absorption characteristics in hydrothermally grown Al doped ZnO thin films* Optical Materials Volume 98, December 2019, 109495
[18] Muaz, A. K. M., Hashim, U., Ibrahim, F., Thong, K. L., Mohktar, M. S., & Liu, W. W. "Effect of annealing temperatures on the morphology, optical and electrical properties of TiO 2 thin films synthesized by the sol–gel method and deposited on Al/TiO 2/SiO 2/p-Si." *Microsystem Technologies* 22 (2016): 871-881.
[19] Kumar, Sanjeev, N. K. Verma, and M. L. Singla. "Size dependent reflective properties of TiO2 nanoparticles and reflectors made thereof." *Digest Journal of Nanomaterials and Biostructures* 7.2 (2012): 607-619. J. Breckling, Ed., *The Analysis of Directional Time Series: Applications to Wind Speed and Direction*, ser. Lecture Notes in Statistics. Berlin, Germany: Springer, 1989, vol. 61.
[20] Cortes, A., Gomez, H., Marotti, R.E., Riveros, G., Dalchiele, E.A., 2004. Grain size dependence of the band gap in chemical bath deposited CdS thin films. Solar Energy Materials & Solar Cells 82, 21–34.Devi, R., Purkayastha, P., Kalita, P. K., & Sarma, B. K. "Synthesis of nanocrystalline CdS thin films in PVA matrix." Bulletin of Materials Science 30.2 (2007).
[21] A.K. Kunti, M. Chowdhury, S.K. Sharma, M. Gupta, R.J. Chaudhary, Thin Solid Films 629, 79 (2017). M. Wegmuller, J. P. von der Weid, P. Oberson, and N. Gisin, "High resolution fiber distributed measurements with coherent OFDR," in Proc. ECOC'00, 2000, paper 11.3.4, p. 109.
[22] T.S. Moss, Proc. Phys. Soc. B 67, 775-782 (1954)
[23] C.M. Maghanga, G.A. Niklasson, C.G. Grangvist, Thin Solid Films 518, 1254-1258 (2009)